Copy
RM E56A31

C2

NACA RM E56A31

NACA

RESEARCH MEMORANDUM

GAS-TO-BLADE HEAT-TRANSFER COEFFICIENTS AND TURBINE HEAT-REJECTION RATES FOR A RANGE OF ONE-SPOOL COOLED-TURBINE ENGINE DESIGNS

By Henry O. Slone and Jack B. Esgar

Lewis Flight Propulsion Laboratory
Cleveland, Ohio

NATIONAL ADVISORY COMMITTEE
FOR AERONAUTICS

WASHINGTON

May 14, 1956

NACA RM E56A31

NATIONAL ADVISORY COMMITTEE FOR AERONAUTICS

RESEARCH MEMORANDUM

GAS-TO-BLADE HEAT-TRANSFER COEFFICIENTS AND TURBINE HEAT-REJECTION RATES FOR A RANGE OF ONE-SPOOL COOLED-TURBINE ENGINE DESIGNS

By Henry O. Slone and Jack B. Esgar

SUMMARY

In order to calculate cooled turbine blade temperatures, coolant temperature rises, and cooled engine performance for a given general type of turbine design, gas-to-blade heat-transfer coefficients and turbine heat-rejection rates must be known. Therefore, gas-to-blade heat-transfer coefficients and turbine heat-rejection rates were obtained for a wide range of one-spool turbojet engine designs believed to be representative of engines that will employ turbine cooling. Both one- and two-stage turbine designs were considered having turbine-inlet temperatures of 2460° and 2800° R. The values of heat-transfer coefficient and heat-rejection rate were calculated for fixed values of turbine tip diameter and turbine blade aspect ratio, assigned limiting blade temperatures, flight Mach numbers from 0.8 to 3.0, altitudes from 50,000 to 80,000 feet, and sea-level compressor equivalent weight flows from 20 to 35 pounds per second per square foot. Equations are presented, however, which correct the values of heat-transfer coefficient or heat-rejection rate or both determined in this analysis for other values of turbine tip diameter, blade aspect ratio, limiting blade temperature, flight Mach number, and altitude.

The values of heat-transfer coefficient and heat-rejection rates are applicable to both liquid- and air-cooled turbines. The effects of sea-level compressor pressure ratio, flight Mach number, compressor equivalent weight flow, and altitude on the total heat rejected from a cooled turbine was studied. In addition, values of heat-transfer coefficients and heat-rejection rates were obtained for a particular cooled turboprop engine design for comparison with a turbojet engine operating at the same conditions.

INTRODUCTION

The gas-to-blade heat-transfer coefficients and turbine heat-rejection rates that are required in the evaluation of various air- and

liquid-cooled turbine engines are presented herein for a wide range of engine designs and operating conditions. The values presented are first-order approximations and can be used for determining average cooled blade temperatures, coolant temperature rises, heat-exchanger requirements, and cooled engine performance for a given general type of turbine design.

Air-cooled turbine blade temperatures can be calculated by the methods of references 1 and 2 once the gas-to-blade heat-transfer coefficients are known, and liquid-cooled turbine blade temperatures can be obtained by the methods of reference 3. (It should be noted that the methods of refs. 1 and 3 also require knowledge of the blade-to-coolant heat-transfer coefficient. Information on these coefficients, however, is not within the scope of the present investigation.) Once the heat-rejection rates are known, temperature gradients within liquid-cooled turbine blades can be determined by the procedure of reference 4. These heat-rejection rates are also necessary in calculating cooled engine performance by the methods in references 5 and 6.

In the past it has been necessary to determine average gas-to-blade heat-transfer coefficients for cooled turbine blades by methods similar to that presented in reference 7. The use of these methods requires that the blade size and geometry, the turbine velocity diagrams, the velocity distribution around the turbine blades, and the density of the combustion gases at the turbine be known. Therefore, the use of reference 7 to calculate heat-transfer coefficients and thus heat-rejection rates for a large number of turbine designs can become quite tedious. It is possible, however, to relate turbine geometry and velocity diagrams to given types of turbine designs such as those discussed in references 8 and 9. In this way, a simplified calculation method can be devised to provide a first-order approximation of the heat-transfer rates associated with a given general type of turbine design.

The purpose of this report is to present gas-to-blade heat-transfer coefficients and cooled turbine heat-rejection rates that can be expected in turbine engines for wide ranges of engine conditions and engine configurations. The results are presented for one-spool turbojet engines having sea-level static compressor pressure ratios from 4 to 12, turbine-inlet temperatures of 2460° and 2800° R, sea-level compressor equivalent weight flows from 20 to 35 pounds per second per square foot, flight Mach numbers from 0.80 to 3.0, and flight altitudes from 50,000 to 80,000 feet. In addition, a comparison is made between the gas-to-blade heat-transfer coefficients and heat-rejection rates of turboprop and turbojet engines at a Mach number of 0.8 at sea level for a compressor pressure ratio of 12 and a turbine-inlet temperature of 2460° R.

The values of gas-to-blade heat-transfer coefficients and heat-rejection rates are applicable to both liquid- and air-cooled turbines, and the results can be used for turbine-inlet temperatures different from those presented by straight-line interpolations. Both one- and two-stage turbine designs are considered.

[redacted]

ANALYTICAL PROCEDURES

The present analysis presents gas-to-blade heat-transfer coefficients and heat-rejection rates for a range of one-spool turbojet engine designs utilizing cooled one- and two-stage turbines. The engine designs considered in this analysis are based on the procedures and results of references 8 and 9. Therefore, the same assumptions used in those references are again applied, along with additional assumptions required to facilitate the required calculations. The symbols used in this report are listed in appendix A, and all assumptions are given in appendix B.

In additon, for purposes of comparison, the gas-to-blade heat-transfer coefficients and heat-rejection rates are obtained for a turboprop engine design. The range of engine conditions and aerodynamic limits assigned to the turbojets and turboprop are believed to be representative of the type of engine operation and design to be expected for engines using turbine cooling. Calculations were made for the following assigned values:

Variable or assigned constant	Turbojet		Turboprop
Number of turbine stages	1	2	3
Flight Mach number	0.8 to 3.0	0.8 to 3.0	0.8
Flight altitude	50,000 to 80,000 ft	Sea level and 50,000 to 80,000 ft	Sea level
Sea-level compressor pressure ratio	4 to 6	6 to 12	12
Turbine-inlet temperature, $^{\circ}R$	2460 and 2800	2460 and 2800	2460
Maximum Mach number at turbine rotor (hub) inlet	0.80	0.60	0.60
Turbine-exit critical axial-velocity ratio	0.70	0.50	0.50
Compressor adiabatic efficiency	0.85	0.85	0.85
Turbine adiabatic efficiency	0.85	0.85	0.85
Primary-combustor pressure ratio	0.95	0.95	0.95
Turbine rotor and stator blade solidity	1.5	1.5	1.5
Stator blade aspect ratio	2.0	2.0	2.0
Rotor blade aspect ratio	2.5	2.5	2.5
Turbine diameter, in.	30	30	30
Average cooled stator blade temperature, $^{\circ}R$	1800	1800	1800
Average cooled rotor blade temperature, $^{\circ}R$	1600	1600	1600
Compressor tip speed, ft/sec	1100	1100	900

Turbine Design

References 8 and 9 were used to obtain the various turbine designs by first specifying the following compressor design parameters: compressor-inlet hub-tip radius ratio $(r_h/r_t)_C$, 0.4; sea-level static compressor equivalent blade tip speed $U_{t,C}/\sqrt{\theta_1}$, 1100 feet per second for turbojet engines and 900 feet per second for the turboprop engine; a range of sea-level static compressor equivalent weight flow $(w_C\sqrt{\theta_1}/A_C\delta_1)_{sl}$, from 20 to 35 pounds per second per square foot for the turbojet engines, and a value of 25 pounds per second per square foot for the turboprop engine. The values of $U_{t,C}/\sqrt{\theta_1} = 900$ feet per second and $(w_C\sqrt{\theta_1}/A_C\delta_1)_{sl} = 25$ pounds per second per square foot chosen for the turboprop engine design were assumed to be more representative than the higher values assumed for the turbojet engines. In order to determine the effects of compressor-inlet temperature (as affected by flight speed and altitude) on compressor equivalent weight flow and pressure ratio at conditions different from sea-level static conditions, it is necessary to specify an engine operating line on a compressor performance map. For this analysis, the performance map of a typical high-output transonic compressor with a constant-mechanical-speed engine operating line was assumed. For simplicity, the same compressor map and engine operating line were used for both the turbojet engine designs and the turboprop engine design.

By use of the assigned values of the compressor design parameters, compressor pressure ratio, turbine aerodynamic limits, and engine temperature ratio corresponding to the assigned values of turbine-inlet temperature, the turbine equivalent weight flow $w_T\sqrt{\theta_1}/A_T\delta_1$, and last-stage hub-tip ratio or hub-tip-radius ratio for a one-stage turbine were obtained from the turbine charts of reference 8 for a flight Mach number of 2.0 in the stratosphere. It can be shown from a study of references 8 and 9 that for constant-mechanical-speed operation and constant turbine-inlet temperature the turbine will operate at or near the design point for a wide range of flight Mach numbers and altitudes. Therefore, the turbine designs considered herein are applicable to the range of flight conditions investigated. Reference 9 was used to evaluate the turbine hub-tip radius ratio for the first-stage turbine of the two-stage turbine designs. For the turboprop engine design, the procedures of reference 9 were used.

Gas-to-Blade Heat-Transfer Coefficient

The average Nusselt number Nu from which the average gas-to-blade heat-transfer coefficient h is obtained was determined by use of the following correlation equation (ref. 10):

$$Nu = \overline{F}\,(Re)^z(Pr)^{1/3} \qquad (1)$$

where the dimension l_o/π is the reference length in Nu and Re, and $\overline{F}$ and z are functions of the transition ratio and Euler number of the blade. When an actual blade profile is available, the values of transition ratio and Euler number may be determined from the velocity distribution around the blade profile. In the present study, however, the actual blade profiles are unknown for the various turbine designs presented herein. The values of $\overline{F}$ and z (eq. (1)) were obtained from reference 10. For the rotor blades, $\overline{F} = 0.092$ and $z = 0.70$. These values of $\overline{F}$ and z were obtained by analyzing ten blade profiles, including both impulse and reaction blades, and evaluating average values of $\overline{F}$ and z. Since stator blades are reaction-type blades, the values used were obtained experimentally in a cascade of reaction blades (ref. 10). The values are $\overline{F} = 0.688$ and $z = 0.52$.

The Reynolds number of equation (1) may be written as

$$\mathrm{Re} = \left(\frac{w\sqrt{T''}}{Ap''}\right)_T \left(\frac{p''}{\sqrt{T''}}\right)_T \left(\frac{T_g}{T_b}\right) \left(\frac{l_o/\pi}{\mu g}\right) \tag{2}$$

If an average Mach number of 0.70 through the blade channel is assumed, the parameter $(w\sqrt{T''}/Ap'')_T$ may be evaluated from reference 11.

A value of 0.70 for the Mach number is consistent with the turbine designs of this analysis. However, higher Mach numbers would not change the parameter $(w\sqrt{T''}/Ap'')_T$ much. A change of Mach number from 0.70 to 1.0 increases $(w\sqrt{T''}/Ap'')_T$ by approximately 8 percent. The values of p''_T and T''_T used in equation (2) are constant through a rotor row (neglecting heat-transfer effects) and were calculated at the stage exit. The static temperature T_g was a calculated mean static temperature. Once the Reynolds number was evaluated from equation (2), equation (1) was used to obtain the gas-to-blade heat-transfer coefficient h. The Prandtl number and other gas physical properties were based on the blade temperature.

Heat-Rejection Rate

The heat per pound of gas Q/w_T rejected within a cooled turbine stage is

$$\frac{Q}{w_T} = \frac{hS\,(T_{g,e} - T_{b,av})}{w_T} \tag{3}$$

where the blade surface area is

$$S = l_o bN \tag{4}$$

[redacted]

and the turbine gas-flow rate w_T may be expressed as

$$w_T = \left(\frac{w_T\sqrt{\theta_1}}{A_T\delta_1}\right)\left(\frac{\delta_1}{\sqrt{\theta_1}}\right)\left(\frac{\pi D_{t,T}^2}{4}\right) \tag{5}$$

It has been found that the ratio of blade perimeter to blade chord is approximately constant at 2.35. Expressing the blade perimeter l_o, blade length b, and number of blades N, as

$$l_o = 2.35\left(\frac{D_{t,T}}{2AR}\right)\left(1 - \frac{r_h}{r_t}\right)_T \tag{6}$$

$$b = \frac{D_{t,T}}{2}\left(1 - \frac{r_h}{r_t}\right)_T \tag{7}$$

$$N = \pi\sigma\ AR\left[\frac{\left(1 + \frac{r_h}{r_t}\right)_T}{\left(1 - \frac{r_h}{r_t}\right)_T}\right] \tag{8}$$

and combining equations (3) to (8) result in

$$\frac{Q}{w_T} = \frac{2.35\ h\sqrt{\theta_1}(T_{g,e} - T_{b,av})(\sigma)\left[1 - \left(\frac{r_h}{r_t}\right)^2\right]_T}{\delta_1\left(\frac{w_T}{A_T}\frac{\sqrt{\theta_1}}{\delta_1}\right)} \tag{9}$$

From equation (9) it can be seen that the heat-rejection rate from the gases to the turbine is a direct function of the turbine design. The effects of blade solidity σ, hub-tip radius ratio $(r_h/r_t)_T$, and flow per unit of turbine frontal area $\frac{w_T}{A_T}\frac{\sqrt{\theta_1}}{\delta_1}$ can be observed directly from the equation. There are also other effects of the turbine design. As will be shown later, the gas-to-blade heat-transfer coefficient h is a function of the blade perimeter l_o, which can be written in terms of the turbine diameter, aspect ratio, and hub-tip radius ratio, as shown in equation (6). The heat-rejection rates are also influenced by the compressor design, because within specified turbine aerodynamic limits, the compressor pressure ratio, tip speed, and flow capacity determine the

turbine hub-tip-radius ratio and the turbine flow capacity $\frac{w_T}{A_T}\frac{\sqrt{\theta_1}}{\delta_1}$. The turbine hub-tip radius ratio and flow capacity are also affected by the turbine aerodynamic design limits. For this analysis the selected aerodynamic limits used were in accordance with the terms "high-output" applied to one-stage turbine designs and "conservative" applied to multistage turbine designs in reference 8. The values of these limits and assigned values affecting the turbine configuration are given in the table presented earlier in the section ANALYTICAL PROCEDURES.

Corrections of Q/w_T and h for Various Engine and Flight Conditions

As stated in the preceding section, for constant-mechanical-speed operation and constant turbine-inlet temperature the turbine will stay on or near design-point operation for a wide range of flight Mach numbers and altitudes. Heat-rejection rates are affected, however, by flight Mach number, altitude, and variables in turbine geometry that are possible for a specified specific turbine work. The heat-rejection rates calculated for this report can be corrected to account for the following variables:

(1) Flight Mach number

(2) Flight altitude

(3) Turbine diameter (with corresponding change in compressor diameter)

(4) Turbine blade solidity

(5) Turbine blade aspect ratio

(6) Blade temperature

Corrections cannot be made readily for variations in sea-level static compressor pressure ratio, sea-level static compressor flow per unit frontal area, turbine-inlet temperature, or type of turbine design (conservative or high-output).

Methods for correcting h and Q/w_t for flight conditions different from a Mach number of 2.0 in the stratosphere and for turbine geometries and temperatures different from those listed in the table in ANALYTICAL PROCEDURES are derived in appendix C. The correction equation for h is

$$h = h_r\left(\frac{T_{b,r}}{T_b}\right)^{1.7z-0.85}\left[\left(\frac{AR}{AR_r}\right)\left(\frac{2.5}{D_T}\right)\right]^{1-z}\left(\frac{K_p\delta_1}{0.783}\right)^z \qquad (10)$$

[redacted]

The value of K_p can be read from figure 1. Values of $T_{b,r}$, AR_r, and z are listed in table I.

In a similar manner, the corrected heat-rejection rate can be expressed by

$$\frac{Q}{w_T} = \left(\frac{Q}{w_T}\right)_r \left[\left(\frac{AR}{AR_r}\right)\left(\frac{2.5}{D_T}\right)\left(\frac{0.783}{\delta_1}\right)\right]^{1-z} (K_p)^2 \left(\frac{\sigma}{1.5}\right)(K_w)\left(\sqrt{\frac{\theta_1}{1.35}}\right)\left(\frac{T_{b,r}}{T_b}\right)^{1.7z-0.85} \left(\frac{T_{g,e} - T_b}{T_{g,e} - T_{b,r}}\right) \quad (11)$$

Values of $T_{b,r}$, $T_{g,e}$, AR_r, and z can be read from table I, and the values of K_w and K_p can be read from figure 1.

RESULTS AND DISCUSSION

Heat-Transfer Coefficients and Heat-Rejection Rates for Turbojet Engine Designs

Gas-to-blade heat-transfer coefficients h and their corresponding heat-rejection rates Q/w_T are plotted against sea-level compressor pressure ratio in figure 2. The results are presented for a sea-level compressor equivalent weight flow of 35 pounds per second per square foot, a flight Mach number of 2.0, an altitude of 50,000 feet, and turbine-inlet temperatures of 2460° and 2800° R. Results for both turbine stator and rotor blades are shown in figure 2. The ranges of compressor pressure ratios shown in figure 2 cover the types of turbine designs discussed in the section ANALYTICAL PROCEDURES. These turbines are believed to be representative of the types that will be encountered in future high-performance cooled turbojet engines. Therefore, the results are of general value for both liquid- and air-cooled engines.

Aside from the specified values of flight Mach number, altitude, and compressor equivalent weight flow, the values of h and Q/w_T shown in figure 2 were calculated for the specific values of turbine tip diameter, turbine blade solidity, turbine blade aspect ratio, and limiting blade temperature considered in this analysis. By use of equations (10) and (11), however, the values of Q/w_T and h may be corrected to conditions other than those presented. In this way it is believed the results can be useful for a large number of engine configurations and flight conditions.

Gas-to-blade heat-transfer coefficient. - Figures 2(a) and (c) show the value of h increasing for both turbine stator and rotor blades as

the sea-level compressor pressure ratio increases. These trends may be explained by referring to equation (1), which may be written as

$$h \propto \frac{C_5}{\left(1 - \frac{r_h}{r_t}\right)_T^{1-z}} \left(\frac{p''}{\sqrt{T''}}\right)_T^z \tag{12}$$

for specified values of turbine blade aspect ratio and solidity, channel Mach number, and turbine-inlet temperature. As compressor pressure ratio increases, the values of p_T'' and $(r_h/r_t)_T$ increase, and there is a slight reduction in T_T''. Thus, these effects cause h to increase with increasing compressor pressure ratio. Comparison of figures 2(a) and (c) shows that a change in turbine-inlet temperature from 2460° to 2800° R generally results in an increase in h.

Although equation (10) can correct the values of h obtained in this analysis for other values of turbine blade aspect ratio, turbine tip diameter, limiting blade temperature, flight Mach number, and altitude, this equation does not correct for the value of compressor equivalent weight flow used in figure 2. Therefore, values of h were calculated for a range of compressor equivalent weight flows for compressor pressure ratios of 6 (one-stage turbine) and 12 (two-stage turbine) and a turbine-inlet temperature of 2460° R. The results of this calculation are shown in figure 3.

The trends observed in figures 2 and 3 may be used to estimate the values of h at values of compressor pressure ratio, turbine-inlet temperature, and compressor equivalent weight flow not specifically shown on the individual figures. In addition, values of h may be obtained at turbine-inlet temperatures other than those presented herein by a straight-line interpolation.

Heat-rejection rate. - As the sea-level compressor pressure ratio increases, Q/w_T increases (figs. 2(b) and (d)) for the stator of the one-stage turbine and the first stator of the two-stage turbine. The rotor blades of both the one- and two-stage turbines and the second-stage stator blades show decreasing values of Q/w_T as pressure ratio increases. An increase in turbine-inlet temperature from 2460° to 2800° R caused an increase in Q/w_T (figs. 2(b) and (d)). The trends observed in figures 2(b) and (d) for Q/w_T can be explained by writing equation (9) in the following way:

$$\frac{Q}{w_T} = \frac{C_6 h \left[1 - \left(\frac{r_h}{r_t}\right)^2\right]_T}{\frac{w_T\sqrt{\theta_1}}{A_T\delta_1}} (T_{g,e} - T_{b,av}) \tag{13}$$

[redacted]

where the values of turbine blade aspect ratio and solidity, channel Mach number, and turbine-inlet temperature are specified.

From the results shown in reference 8 it can be seen that increasing the compressor pressure ratio for constant equivalent compressor weight flow and compressor tip speed results in an increasing value of $(r_h/r_t)_T$ and a slightly decreasing value of $w_T\sqrt{\theta_1}/A_T\delta_1$. Figures 2(a) and (c) show that the heat-transfer coefficient h increases with compressor pressure ratio. Table I shows that the values of $T_{g,e}$ are independent of compressor pressure ratio for the stator blades of the one-stage turbine and for the first stage of the two-stage turbine. Thus the temperature difference $T_{g,e} - T_{b,av}$ remains constant for the first-stage stator blades as compressor pressure ratio increases. The over-all result is that Q/w_T increases in a manner similar to the heat-transfer coefficient h, but to a smaller degree, as the compressor pressure ratio is increased (figs. 2(b) and (d)).

Table I shows a decrease in $T_{g,e}$ for the rotor blades and second-stage stator blades as compressor pressure ratio increases. Thus, for the constant value of $T_{b,av}$, the temperature difference $T_{g,e} - T_{b,av}$ decreases more than the combination of other terms in equation (13) increases. As a result, the values of Q/w_T for the rotor blades and second-stage stator blades decrease as compressor pressure ratio changes from 4 to 12. It is possible that if different values were chosen for $T_{b,av}$ the trends shown in figures 2(b) and (d) might be altered.

Total Heat-Rejection Rates for Various Turbojet Engine and Flight Conditions

The total heat-rejection rate $(Q/w_T)_{tot}$, which is the sum of the heat-rejection rates for the turbine stator and rotor blades, is required in the evaluation of engine performance. Figures 4 and 5 show the effects of sea-level compressor pressure ratio, flight Mach number, sea-level compressor equivalent weight flow, and altitude on $(Q/w_T)_{tot}$. The values of $(Q/w_T)_{tot}$ presented in figure 4(a) were obtained from figures 2(b) and (d). Then, equation (10) and figures 2(b) and (d) were used to obtain figures 4(b) and 5(b). The methods discussed in the ANALYTICAL PROCEDURES were used to obtain figure 5(a).

Effect of compressor pressure ratio. - As the sea-level compressor pressure ratio is changed from 4 to 6 for the one-stage turbine, the increase in $(Q/w_T)_{tot}$ for a given turbine-inlet temperature is about 5 percent (fig. 4(a)). For the two-stage turbine, $(Q/w_T)_{tot}$ decreases as the compressor pressure ratio varies from 6 to 12. This decrease in

$(Q/w_T)_{tot}$ is about 7 and 2 percent for turbine-inlet temperatures of 2460° and 2800° R, respectively. As the turbine-inlet temperature rises from 2460° to 2800° R for constant compressor pressure ratio, a noticeable increase in $(Q/w_T)_{tot}$ of about 60 to 70 percent occurs.

Effect of flight Mach number. - The effect of flight Mach number on $(Q/w_T)_{tot}$ is illustrated in figure 4(b) for both one- and two-stage turbines. Since the effect of compressor pressure ratio on $(Q/w_T)_{tot}$ is small (see fig. 4(a)), a compressor pressure ratio of 6 was selected as being representative of one-stage turbines and a pressure ratio of 12 typical for two-stage turbines. Only the turbine-inlet temperature of 2460° R was considered in figure 4(b) because the effect of a 2800° R turbine-inlet temperature on $(Q/w_T)_{tot}$ is clearly indicated in figure 4(a). As the Mach number changed from 0.8 to 3.0, $(Q/w_T)_{tot}$ decreases about 37 and 36 percent for the one- and two-stage turbines, respectively.

Effect of compressor equivalent weight flow. - The results shown in figure 4 were obtained for a sea-level static compressor equivalent weight flow $(w_C\sqrt{\theta_1}/A_C\delta_1)_{sl}$ of 35 pounds per second per square foot. The effect of $(w_C\sqrt{\theta_1}/A_C\delta_1)_{sl}$ on $(Q/w_T)_{tot}$ is presented in figure 5(a) for an altitude of 50,000 feet and compressor pressure ratios of 6 (one-stage turbine) and 12 (two-stage turbine).

Figure 5(a) shows that values of $(Q/w_T)_{tot}$ for one- and two-stage turbines are affected differently by $(w_C\sqrt{\theta_1}/A_C\delta_1)_{sl}$. For the one-stage turbine, $(Q/w_T)_{tot}$ remains practically constant as $(w_C\sqrt{\theta_1}/A_C\delta_1)_{sl}$ increases from 20 to 35 pounds per second per square foot. The same change in $(w_C\sqrt{\theta_1}/A_C\delta_1)_{sl}$ results in a decrease of about 16 percent in $(Q/w_T)_{tot}$ for the two-stage turbine. These differences in behavior for the one- and two-stage turbines may be attributed to the variations in the turbine hub-tip radius ratios and equivalent weight flows that appear in equation (9).

Effect of altitude. - An altitude of 50,000 feet was used in the presentation of figures 4 and 5(a). The effect of altitude on $(Q/w_T)_{tot}$ is shown in figure 5(b). As the altitude is changed from 50,000 to 80,000 feet, $(Q/w_T)_{tot}$ increases about 75 percent for both the one- and two-stage turbines. This increase in the total heat-rejection rate with increasing altitude may easily be explained by referring to equation (11). As altitude is increased, δ_1 decreases because of the lower atmospheric pressure, and thus the total heat-rejection rate increases.

Heat-Transfer Coefficients and Heat-Rejection Rates for Turboprop Engine Design

As a matter of interest, values of the gas-to-blade heat-transfer coefficient h and the total heat-rejection rate $(Q/w_T)_{tot}$ were obtained for a turboprop engine design having a turbine-inlet temperature of 2460° R, a sea-level compressor pressure ratio of 12, and a flight Mach number of 0.8 at sea level. Other assigned values necessary for these calculations are listed in the table in the section ANALYTICAL PROCEDURES.

The particular turboprop engine design considered in this analysis required three turbine stages. Since the inlet gas temperature of the third stage was approximately the same as the limiting assigned blade temperature of the stator and rotor blades, it was assumed that the third turbine stage required no cooling.

The total heat-rejection rate $(Q/w_T)_{tot}$, which is the sum of the first and second turbine stages, is 8.96 Btu per pound for the turboprop engine. The heat-transfer coefficients are 0.158 and 0.165 Btu/(sec)(sq ft)(°F) for the first-stage stator and rotor blades, respectively. Values of 0.0588 and 0.0632 Btu/(sec)(sq ft)(°F) were obtained for the second-stage stator and rotor blades.

In order to compare the values of $(Q/w_T)_{tot}$ and h obtained for the turboprop engine with values obtained for a turbojet engine, calculations were made for a turbojet having the same turbine-inlet temperature and compressor pressure ratio and operating at the same flight conditions as the turboprop. The results are shown in the following table:

Engine	Total heat-rejection rate, $(Q/w_T)_{tot}$, Btu/lb	Gas-to-blade heat-transfer coefficient, h, Btu/(sec)(sq ft)(°F)			
		First stage		Second stage	
		Stator	Rotor	Stator	Rotor
Turboprop	8.96	0.158	0.165	0.0588	0.0632
Turbojet	6.23	.091	.119	.046	.061

The heat-transfer coefficients are higher for the turboprop than for the turbojet primarily because of higher hub-tip radius ratios in the turboprop, which for a given blade aspect ratio and solidity result in smaller blades. These higher heat-transfer coefficients in turn are reflected in higher heat-rejection rates. There is a smaller difference between heat-rejection rates in turboprop and turbojet engines than between heat-transfer coefficients because the heat-transfer surface area is smaller in turboprops because of the higher hub-tip radius ratios.

CONCLUSIONS

The results of this study are intended to be useful in the evaluation of cooled turbine blade temperatures and engine performance for various air- and liquid-cooled turbojet engines over wide ranges of engine designs and operating conditions.

Values of gas-to-blade heat-transfer coefficients and heat-rejection rates were calculated for turbine-inlet temperatures of 2460° and 2800° R, a flight Mach number of 2.0 at an altitude of 50,000 feet, sea-level compressor equivalent weight flows from 20 to 35 pounds per second per square foot, and fixed values of turbine tip diameter, turbine blade aspect ratio, and limiting blade temperature. Equations are presented which correct the values determined in this analysis for other flight Mach numbers, altitudes, turbine tip diameters, blade aspect ratios, and limiting blade temperatures. By use of the values of gas-to-blade heat-transfer coefficients and total heat-rejection rates presented herein as a first-order approximation, cooled turbine blade temperatures and cooled engine performance may be evaluated for a number of turbine designs. In addition, the values of heat-transfer coefficient and total heat-rejection rate determined for a representative cooled turboprop engine may be used as a guide for evaluating heat-transfer coefficients and total heat-rejection rates for other turboprop designs.

The results of this analysis may be summarized as follows:

1. For a given sea-level compressor pressure ratio, a change in turbine-inlet temperature from 2460° to 2800° R generally results in an increase in both the gas-to-blade heat-transfer coefficient and the heat-rejection rate.

2. Gas-to-blade heat-transfer coefficients for both turbine stator and rotor blades increase as the sea-level compressor pressure ratio changes from 4 to 12.

3. For a given turbine-inlet temperature, the total heat-rejection rate increases about 5 percent as the sea-level compressor pressure ratio changes from 4 to 6 (one-stage turbine). A decrease of about 7 percent in the total heat-rejection rate occurs as sea-level compressor pressure ratio increases from 6 to 12 (two-stage turbine).

4. A change in flight Mach number from 0.8 to 3.0 results in about 37- and 36-percent decreases in the total heat-rejection rates for one- and two-stage turbines, respectively, for a given compressor pressure ratio and turbine-inlet temperature.

5. A change in the sea-level static compressor equivalent weight flow $(w_c\sqrt{\theta_1}/A_c\delta_1)_{sl}$ from 20 to 35 pounds per second per square foot

causes no significant change in $(Q/w_T)_{tot}$ for one-stage turbines. A decrease of about 16 percent in $(Q/w_T)_{tot}$ occurs for the two-stage turbines.

6. As the altitude is increased from 50,000 to 80,000 feet, $(Q/w_T)_{tot}$ increases about 75 percent for both the one- and two-stage turbines.

7. Both the gas-to-blade heat-transfer coefficients and the total heat-rejection rate are higher for a turboprop than for a turbojet operating at the same conditions as the turboprop engine.

Lewis Flight Propulsion Laboratory
National Advisory Committee for Aeronautics
Cleveland, Ohio, February 2, 1956

APPENDIX A

SYMBOLS

The following symbols are used in this report:

A	flow area, sq ft
A_C	compressor frontal area, sq ft
A_T	turbine frontal area, sq ft
AR	turbine blade aspect ratio, b/c
b	turbine blade span or length, ft
C_1, C_2, C_3 C_4, C_5, C_6	constants
c	blade chord, ft
c_p	specific heat at constant pressure based on blade temperature, Btu/(lb)($^\circ$F)
D	diameter, ft
$\overline{F}$	mean coefficient in eq. (1)
g	acceleration due to gravity, 32.174 ft/sec^2
h	average gas-to-blade heat-transfer coefficient, Btu/(sec)(sq ft)($^\circ$F)
K	correction factor
k	gas thermal conductivity based on blade temperature, Btu/(sec)(ft)($^\circ$F)
l_o	turbine blade outside perimeter, ft
N	number of blades
Nu	average Nusselt number, $(hl_o/\pi)/k$
Pr	Prandtl number of gas based on blade temperature, $c_p\mu g/k$

p	pressure, lb/sq ft
Q/w_T	heat-rejection rate, Btu/lb
Re	average Reynolds number of gas, $\left(\frac{w_T l_c/\pi}{A_T \mu_g}\right)\left(\frac{T_g}{T_b}\right)$
r	radius, ft
S	turbine blade surface area, sq ft
T	temperature, $^{\circ}R$
U	blade velocity, ft/sec
w	weight-flow rate, lb/sec
z	exponent of Reynolds number (eq. (1))
δ_1	ratio of total pressure at compressor inlet to NACA standard sea-level pressure, $p_1'/2116$
θ	ratio of total temperature to NACA standard sea-level temperature, $T'/518.7$
μ	gas viscosity based on blade temperature, slugs/(sec)(ft)
σ	turbine blade solidity, $cN/\pi D_m$

Subscripts:

av	average
b	blade, or referring to blade temperature
C	compressor
e	effective
g	gas
h	hub
m	mean
p	corrected for pressure ratio
r	denotes reference values used in analysis
sl	sea-level static

4003

T turbine

t tip

tot total

w corrected for weight flow

1 compressor inlet

2 compressor outlet

3 turbine inlet

Superscripts:

' gas stagnation conditions

" gas stagnation state relative to stator or rotor blades

[redacted]

APPENDIX B

ASSUMPTIONS

The following assumptions were made to facilitate the analysis:

(1) Turbine design
  (a) Free-vortex velocity distribution
  (b) Simplified radial equilibrium
  (c) No radial variation in stagnation state relative to stator
  (d) Hub, mean, and tip radii constant in value from entrance to exit of each rotor blade row
  (e) Work split of 65 to 35 percent for two-stage turbojet engines
  (f) Hub-tip radius ratio of last stage of turbine in turboprop of 0.60

(2) Constant mechanical speed for all flight conditions
  (a) Compressor tip speed of 1100 feet per second for turbojet engines
  (b) Compressor tip speed of 900 feet per second for turboprop engines

(3) Negligible mechanical friction

(4) Negligible pumping power of auxiliary heat exchangers (if any)

(5) Single-spool turbojet and turboprop engines

(6) Optimum jet velocity for turboprop engine

(7) Equivalent specific air flow $\frac{w_c}{A_c}\frac{\sqrt{\theta_1}}{\delta_1}$ at sea level of 25 pounds per second per square foot for turboprop engine design

4003

[redacted]

APPENDIX C

DERIVATION OF EQUATIONS FOR CORRECTIONS OF Q/w_T AND h FOR VARIOUS ENGINE AND FLIGHT CONDITIONS

From equations (1) and (2) the gas-to-blade heat-transfer coefficient h can be written

$$h = \frac{\bar{F}k}{\left(\frac{l_o}{\pi}\right)^{1-z}}\left[\left(\frac{w\sqrt{T''}}{Ap''}\right)_T\left(\frac{p''}{\sqrt{T''}}\right)_T\left(\frac{T_g}{T_b}\right)\left(\frac{1}{\mu g_c}\right)\right]^z (Pr)^{1/3} \tag{C1}$$

The gas fluid properties can be written as a function of temperature

$$k = C_1 T_b^{0.85} \tag{C2}$$

$$\mu = C_2 T_b^{0.7} \tag{C3}$$

$$Pr \approx C_3 \tag{C4}$$

For a given turbine design

$$\frac{p_T''}{\delta_1} \propto \frac{p_2'}{p_1'} \tag{C5}$$

For a constant mechanical speed the compressor pressure ratio p_2'/p_1' is dependent upon the compressor equivalent speed $N/\sqrt{\theta_1}$, which in turn is dependent upon altitude and flight Mach number. The variation of p_2'/p_1' with flight Mach number and altitude relative to the value of a Mach number of 2.0 in the stratosphere is K_p, which is defined as

$$K_p = \frac{(p_2'/p_1')}{(p_2'/p_1')_r} \tag{C6}$$

Values of K_p are shown in figure 1 for a range of Mach number from zero to 3 for sea level and in the stratosphere. This figure was evaluated from the operating line of the performance map for a transonic compressor mentioned in the section ANALYTICAL PROCEDURES.

Equation (C5) can now be written

$$\delta_1 K_p = C_4 p_T'' \tag{C7}$$

By use of equations (6) and (C1) to (C7), an expression can be written that relates heat-transfer coefficients for different engine and flight conditions as follows:

$$h = h_r \left(\frac{T_{b,r}}{T_b}\right)^{1.7z-0.85} \left[\left(\frac{AR}{AR_r}\right)\left(\frac{D_{T,r}}{D_T}\right)\right]^{1-z} \left(\frac{K_p\delta_1}{\delta_{1,r}}\right)^z \qquad (C8)$$

There are no effects of $\overline{F}$, T_T'', T_g, or $(w\sqrt{T''}/Ap'')_T$ in equation (C8). These values cancel out because they are constant for the assumptions employed herein. By incorporating values of $\delta_{1,r}$ and $D_{T,r}$ used in this investigation, equation (C8) becomes

$$h = h_r \left(\frac{T_{b,r}}{T_b}\right)^{1.7z-0.85} \left[\left(\frac{AR}{AR_r}\right)\left(\frac{2.5}{D_T}\right)\right]^{1-z} \left(\frac{K_p\delta_1}{0.783}\right)^z \qquad (10)$$

Values of $T_{b,r}$, AR_r, and z are listed in table I.

In a similar manner, equations (9) and (10) can be combined to obtain

$$\frac{Q}{w_T} = \left(\frac{Q}{w_T}\right)_r \left[\left(\frac{AR}{AR_r}\right)\left(\frac{D_{T,r}}{D_T}\right)\left(\frac{\delta_{1,r}}{\delta_1}\right)\right]^{1-z} (K_p)^2 \left(\frac{\sigma}{\sigma_r}\right) \frac{\left(\frac{w_T\sqrt{\theta_1}}{A_T\delta_1}\right)_r}{\left(\frac{w_T\sqrt{\theta_1}}{A_T\delta_1}\right)} \sqrt{\frac{\theta_1}{\theta_{1,r}}} \left(\frac{T_{b,r}}{T_b}\right)^{1.7z-0.85} \left(\frac{T_{g,e} - T_b}{T_{g,e} - T_{b,r}}\right)$$

(C9)

Since the gas flow through the turbine is a function of compressor air flow,

$$\frac{w_T\sqrt{\theta_1}}{A_T\delta_1} = C_5 \frac{w_1\sqrt{\theta_1}}{A_1\delta_1} \qquad (C10)$$

The compressor equivalent flow varies with flight Mach number and altitude in a manner similar to that for compressor pressure ratio. Values of K_w defined as

$$K_w = \frac{\left(\frac{w_1\sqrt{\theta_1}}{A_1\delta_1}\right)_r}{\frac{w_1\sqrt{\theta_1}}{A_1\delta_1}} \qquad (C11)$$

are presented in figure 1.

4003

Substituting reference values in equation (C9) and combining with equations (C10) and (C11) result in

$$\frac{Q}{w_T} = \left(\frac{Q}{w_T}\right)_r \left[\left(\frac{AR}{AR_r}\right)\left(\frac{2.5}{D_T}\right)\left(\frac{0.783}{\delta_1}\right)\right]^{1-z} (K_p)^2 \left(\frac{\sigma}{1.5}\right)(K_w)\left(\sqrt{\frac{\theta_1}{1.35}}\right)\left(\frac{T_{b,r}}{T_b}\right)^{1.7z-0.85}\left(\frac{T_{g,e} - T_b}{T_{g,e} - T_{b,r}}\right) \tag{11}$$

Values of AR_r, $T_{b,r}$, $T_{g,e}$, $T_{b,r}$, and z are listed in table I.

REFERENCES

1. Livingood, John N. B., and Brown, W. Byron: Analysis of Spanwise Temperature Distribution in Three Types of Air-Cooled Turbine Blades. NACA Rep. 994, 1950. (Supersedes NACA RM's E7B11e and E7G30.)

2. Slone, Henry O., Hubbartt, James E., and Arne, Vernon L.: Method of Designing Corrugated Surfaces Having Maximum Cooling Effectiveness Within Pressure-Drop Limitations for Application to Cooled Turbine Blades. NACA RM E54H20, 1954.

3. Livingood, John N. B., and Brown, W. Byron: Analysis of Temperature Distribution in Liquid-Cooled Turbine Blades. NACA Rep. 1066, 1952. (Supersedes NACA TN 2321.)

4. Bartoo, Edward R.: Temperature Drops Through Liquid-Cooled Turbine Blades with Various Cooling-Passage Geometries. NACA RM E55K18, 1956.

5. Esgar, Jack B., and Ziemer Robert R.: Methods for Rapid Graphical Evaluation of Cooled or Uncooled Turbojet and Turboprop Engine or Component Performance (Effects of Variable Specific Heat Included). NACA TN 3335, 1955.

6. Esgar, Jack B., and Slone, Henry O.: Gas-Turbine-Engine Performance when Heat from Liquid-Cooled Turbines is Rejected Ahead of, Within, or Behind the Main Compressor. NACA RM E56B09, 1956.

7. Brown, W. Byron, and Donoughe, Patrick L.: Extension of Boundary-Layer Heat-Transfer Theory to Cooled Turbine Blades. NACA RM E50F02, 1950.

[redacted]

8. Cavicchi, Richard H., and English, Robert E.: Analysis of Limitations Imposed on One-Spool Turbojet-Engine Designs by Compressors and Turbines at Flight Mach Numbers of 0, 2.0, and 2.8. NACA RM E54F21a, 1954.

9. Cavicchi, Richard H., and English, Robert E.: A Rapid Method for Use in Design of Turbines Within Specified Aerodynamic Limits. NACA TN 2905, 1953.

10. Slone, Henry O., and Hubbartt, James E.: Analysis of Factors Affecting Selection and Design of Air-Cooled Single-Stage Turbines for Turbojet Engines. IV - Coolant-Flow Requirements and Performance of Engines Using Air-Cooled Corrugated-Insert Blades. NACA RM E55C09, 1955.

11. Hubbartt, James E., Slone, Henry O., and Arne, Vernon L.: Method for Rapid Determination of Pressure Change for One-Dimensional Flow with Heat Transfer, Friction, Rotation, and Area Change. NACA TN 3150, 1954.

4003

[redacted]

TABLE I. - VALUES REQUIRED FOR HEAT-REJECTION CORRECTIONS

(a) One-stage turbine.

Sea-level compressor pressure ratio, $(p'_2/p'_1)_{sl}$	Turbine-inlet temperature, T'_3, ^oR	Stator				Rotor			
		Reynolds number exponent, z	Reference aspect ratio, AR_r	Reference blade temperature, $T_{b,r}$, ^oR	Effective gas temperature, $T_{g,e}$, ^oR	Reynolds number exponent, z	Reference aspect ratio, AR_r	Reference blade temperature, $T_{b,r}$, ^oR	Effective gas temperature, $T_{g,e}$, ^oR
4	2460	0.52	2.0	1800	2435	0.70	2.5	1600	2293
4	2800	↓	↓	↓	2772	↓	↓	↓	2633
6	2460	↓	↓	↓	2435	↓	↓	↓	2203
6	2800	↓	↓	↓	2772	↓	↓	↓	2551

TABLE I. - Concluded. VALUES REQUIRED FOR HEAT-REJECTION CORRECTIONS

(b) Two-stage turbine.

Sea-level compressor pressure ratio, $(p'_2/p'_1)_{sl}$	Turbine-inlet temperature, T'_3, °R	Stator				Rotor			
		Reynolds number exponent, z	Reference aspect ratio, AR_r	Reference blade temperature, $T_{b,r}$, °R	Effective gas temperature, $T_{g,e}$, °R	Reynolds number exponent, z	Reference aspect ratio, AR_r	Reference blade temperature, $T_{b,r}$, °R	Effective gas temperature, $T_{g,e}$, °R
First stage									
6	2460	0.52	2.0	1800	2435	0.70	2.5	1600	2337
6	2800				2772				2674
8	2460				2435				2310
8	2800				2772				2647
10	2460				2435				2284
10	2800				2772				2622
12	2460				2435				2264
12	2800				2772				2600
Second stage									
6	2460	0.52	2.0	1800	2238	0.70	2.5	1600	2166
6	2800				2581				2513
8	2460				2182				2087
8	2800				2528				2435
10	2460				2133				2021
10	2800				2481				2372
12	2460				2097				1967
12	2800				2442				2316

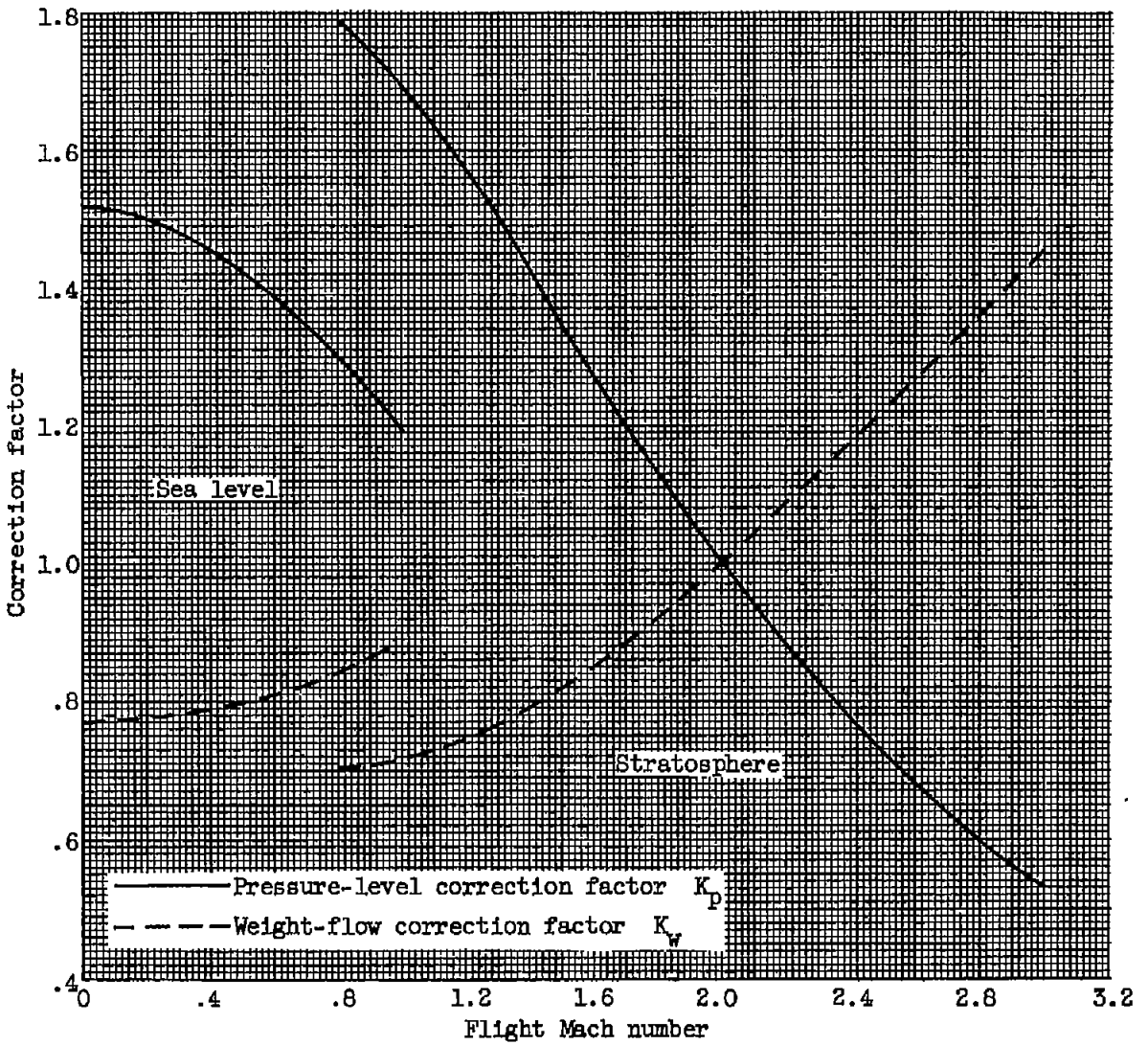

Figure 1. - Correction factors for use in equations (10) and (11).

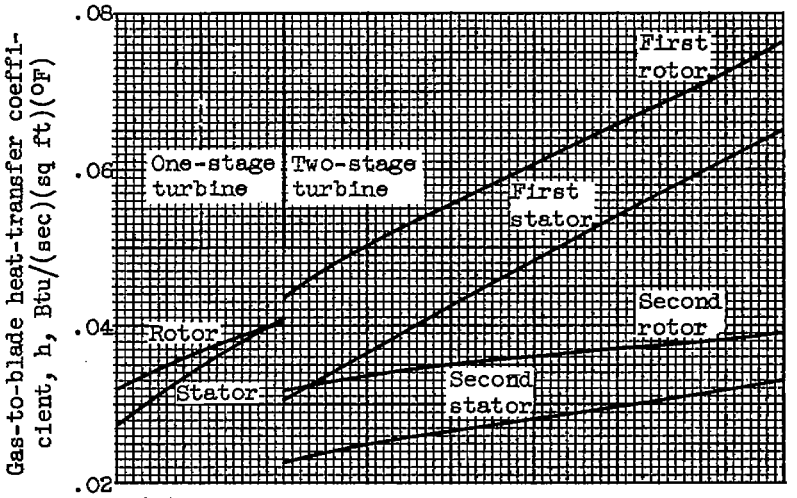

(a) Gas-to-blade heat-transfer coefficient. Turbine-inlet temperature, 2460° R.

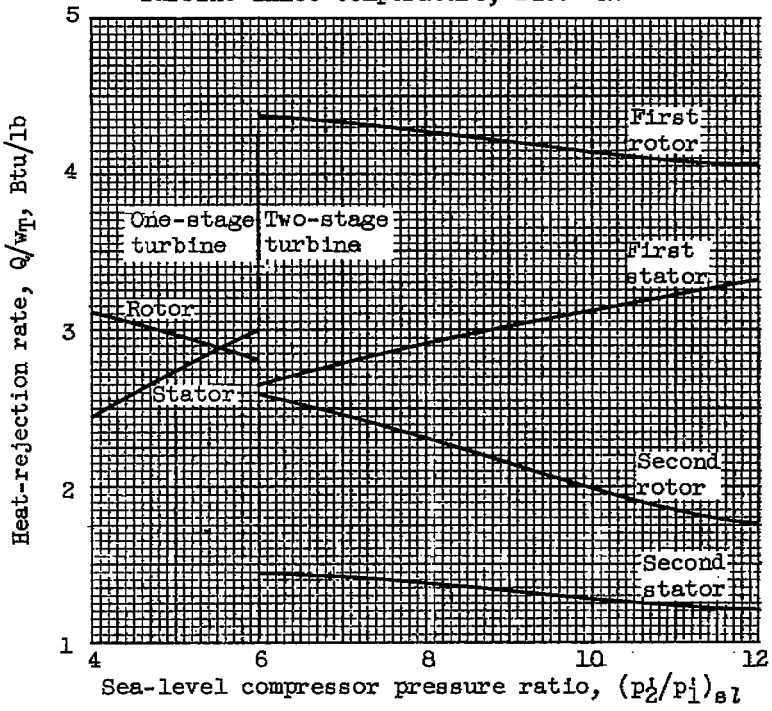

(b) Heat-rejection rate. Turbine-inlet temperature, 2460° R.

Figure 2. - Variation of gas-to-blade heat-transfer coefficient and heat-rejection rate with compressor pressure ratio. Flight Mach number, 2.0; altitude, 50,000 feet; sea-level compressor equivalent weight flow, 35.0 pounds per second per square foot.

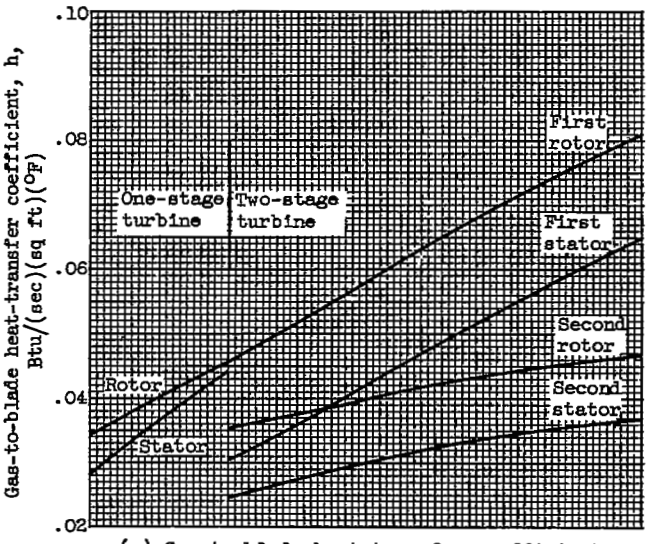

(c) Gas-to-blade heat-transfer coefficient. Turbine-inlet temperature, 2800° R.

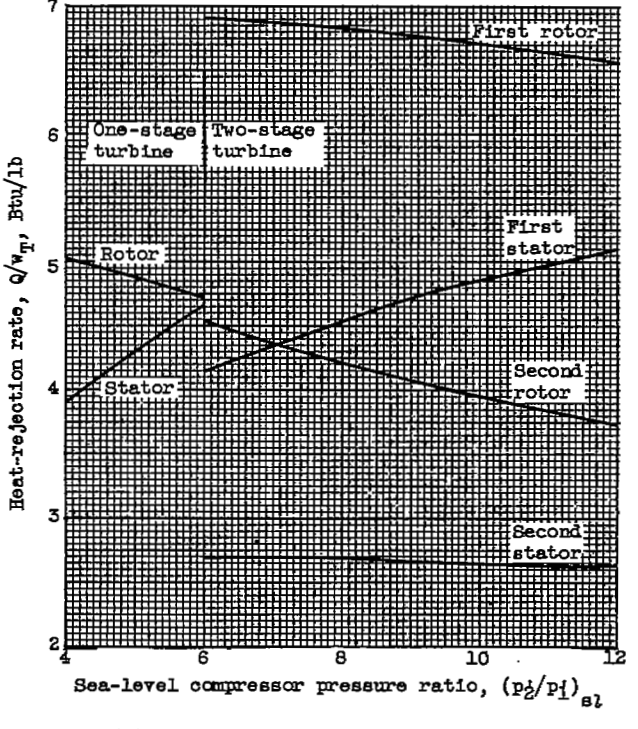

(d) Heat-rejection rate. Turbine-inlet temperature, 2800° R.

Figure 2. - Concluded. Variation of gas-to-blade heat-transfer coefficient and heat-rejection rate with compressor pressure ratio. Flight Mach number, 2.0; altitude, 50,000 feet; sea-level compressor equivalent weight flow, 35.0 pounds per second per square foot.

[redacted]

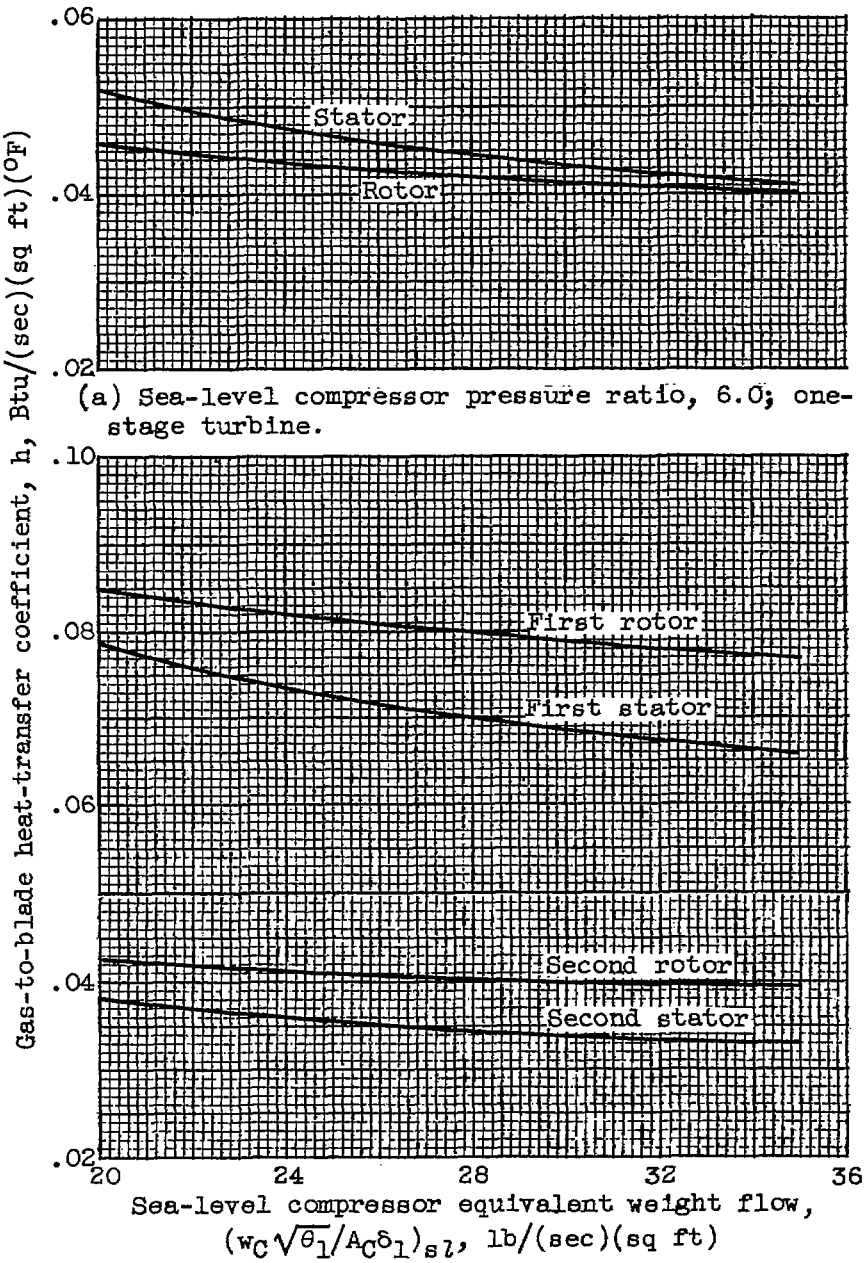

(a) Sea-level compressor pressure ratio, 6.0; one-stage turbine.

(b) Sea-level compressor pressure ratio, 12.0; two-stage turbine.

Figure 3. - Effect of sea-level compressor equivalent weight flow on gas-to-blade heat-transfer coefficient. Turbine-inlet temperature, 2460° R; flight Mach number, 2.0; altitude, 50,000 feet.

[redacted]

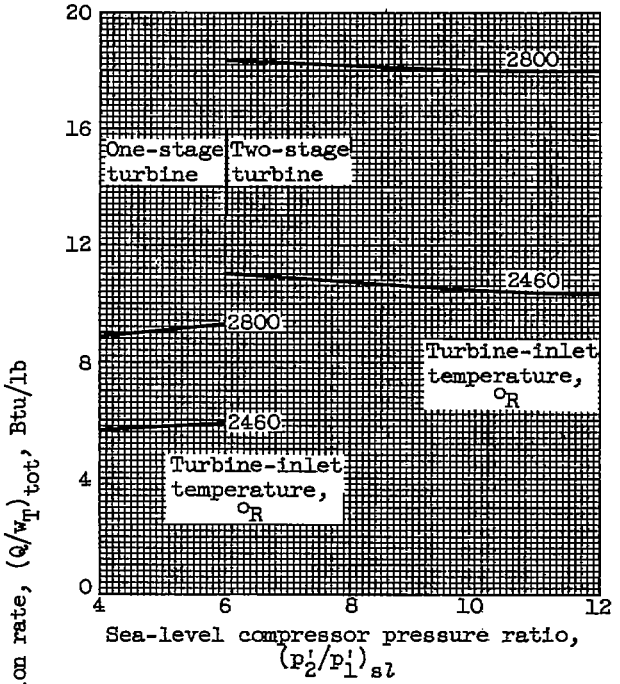

(a) Effect of compressor pressure ratio. Flight Mach number, 2.0.

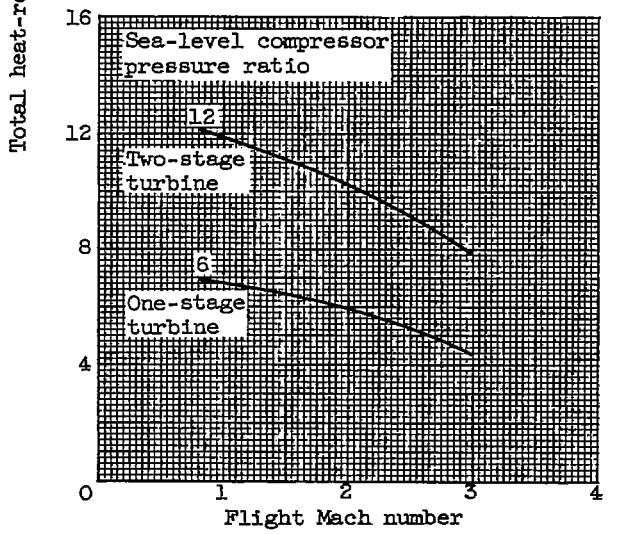

(b) Effect of flight Mach number. Turbine-inlet temperature, 2460° R.

Figure 4. - Effects of sea-level compressor pressure ratio and flight Mach number on total heat-rejection rate. Altitude, 50,000 feet; sea-level compressor equivalent weight flow, 35.0 pounds per second per square foot.

[redacted]

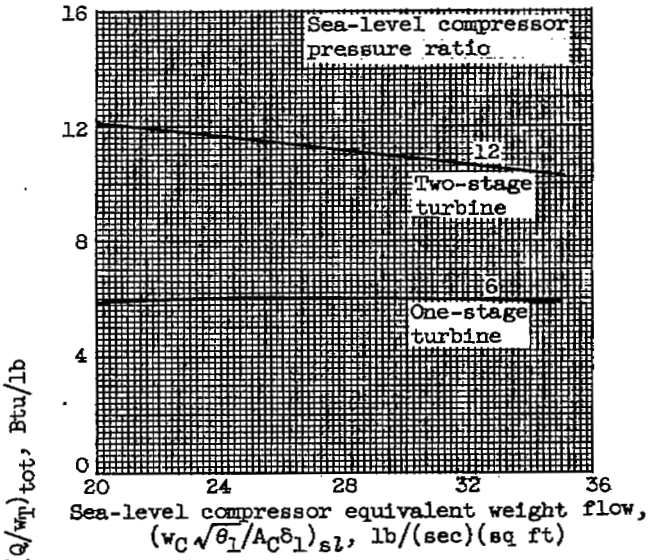

(a) Effect of compressor equivalent weight flow. Altitude, 50,000 feet.

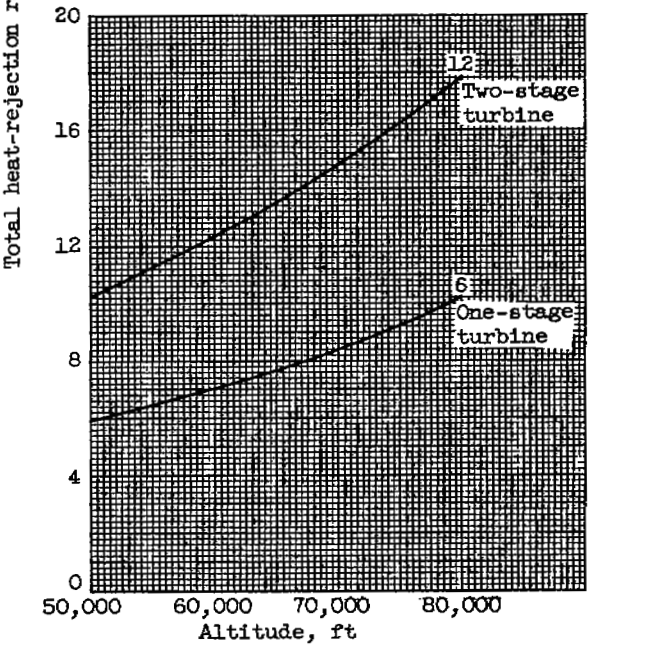

(b) Effect of altitude. Sea-level compressor equivalent weight flow, 35.0 pounds per second per square foot absolute.

Figure 5. - Effects of sea-level compressor equivalent weight flow and altitude on total heat-rejection rate. Flight Mach number, 2.0; turbine-inlet temperature, 2460° R.